Lviv Polytechnic National University

Functional Luminescent Oligoelectrolyte Surfactants, Nanoessemblies, Nanoparticles and Nanolayered Surfaces: Novel Complex Approaches of the Synthesis

A. Zaichenko,
zaichenk@polynet.lviv.ua

The aim of the study:

oligoperoxide based routes of tailored synthesis and functionalization of luminescent and scintillation nanocomposites for biology and medicine

Talk outline

I. The main routes of the synthesis and functionalization of luminescent and scintillation polymeric and mineral nanocomposites

II. Opportunities of biomedical application of luminescent and scintillation nanoparticles for cell detection, tagging and treatment.

I. The main routes of the synthesis and functionalization of luminescent and scintillation functional polymer coated nanocomposites

I. The main routes of the synthesis and functionalization of luminescent and scintillation polymeric and mineral nanoparticles

I.1. Synthesis of polymer based salts and complexes of rare earth elements with oligoperoxide ligands (OMC) and luminescent polymeric nanoparticles (30 – 150nm) via water dispersion polymerization initiated and stabilized by OMC.

I.2. Synthesis of oligoperoxide and derived oligoelectrolyte surfactants containing luminescent fragments as a result of reactions with reactive phosphors.

I.3. Formation of micelle-like assemblies formed by oligoperoxide or oligoelectrolyte surfactants containing organic phosphors in hydrophobic core.

I.4. Synthesis of oligoelectrolyte based nanogels containing coordinated rare earth cations or filled with organic phosphors in the pores.

I. The main routes of the synthesis and functionalization of luminescent and scintillation polymeric and mineral nanoparticles

I.5. Encapsulation of the phosphors (fluorescein, pyrazolyne and others) in the core of functional polymeric nanoparticles via water dispersion polymerization.

I.6. Template synthesis of functionalized mineral nanoparticles of $LaPO_4$, $LuPO_4$, $LuBO_3$, GdF_3, CaF_2, BaF_2 doped with Pr^{+3}, Ce^{+3}, Eu^{+2} and Eu^{+3} and oligoperoxide shell capable of grafting functional polymer chains.

I.1. Copolymerization of unsaturated ditertiary peroxides with functional monomers.

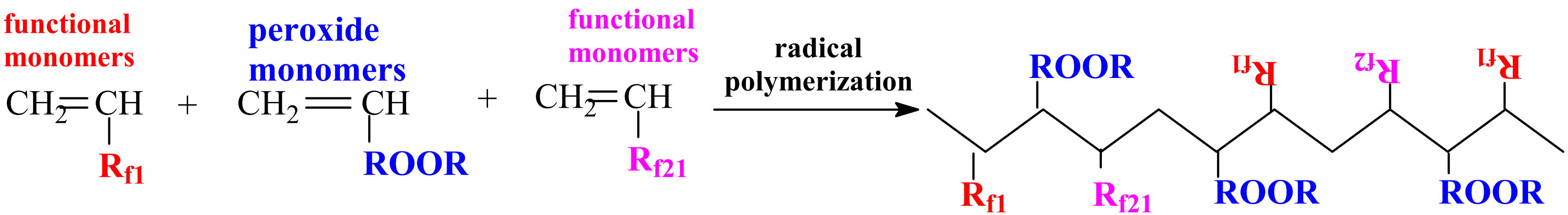

The general structure of surface - active linear oligoperoxides

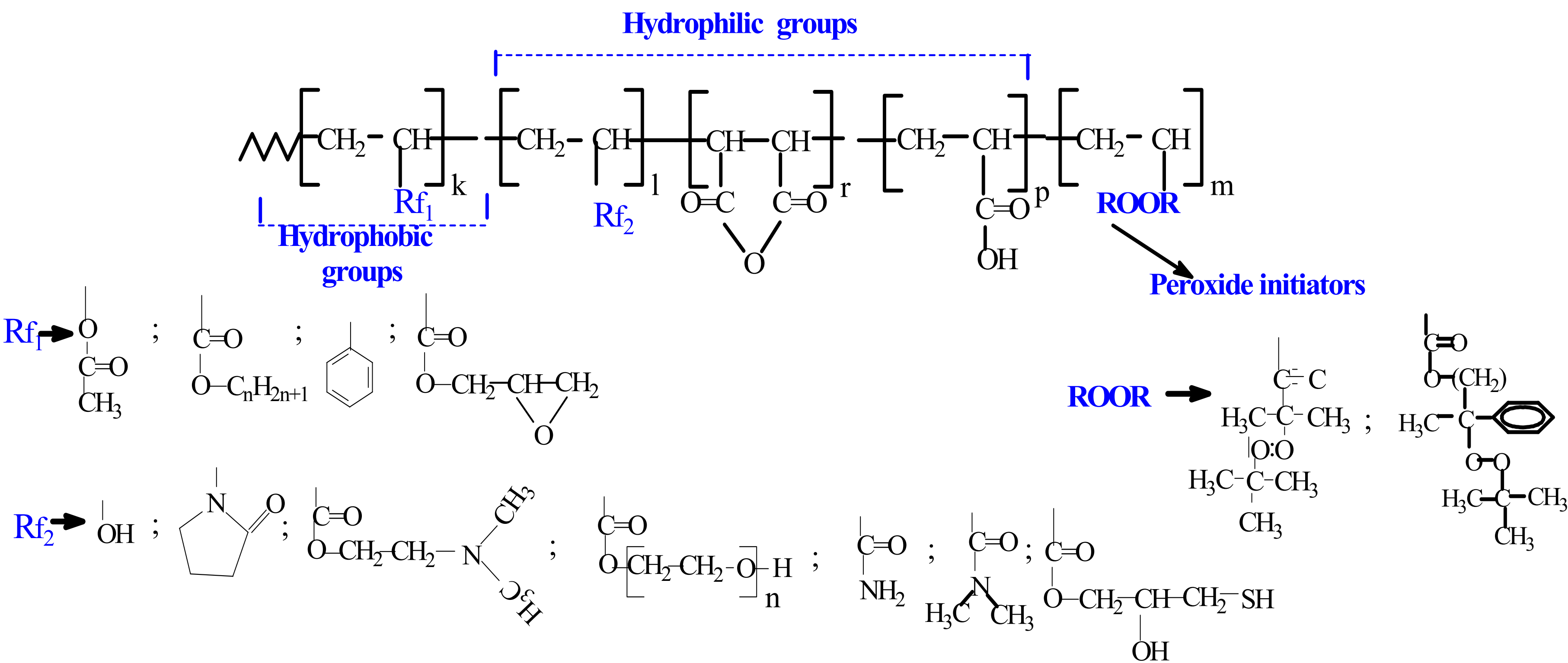

I.1. Coordinating complexes of rare earth elements with oligoperoxide ligands (OMC) and polymeric nanoparticles synthesized via water dispersion polymerization initiated by OMC.

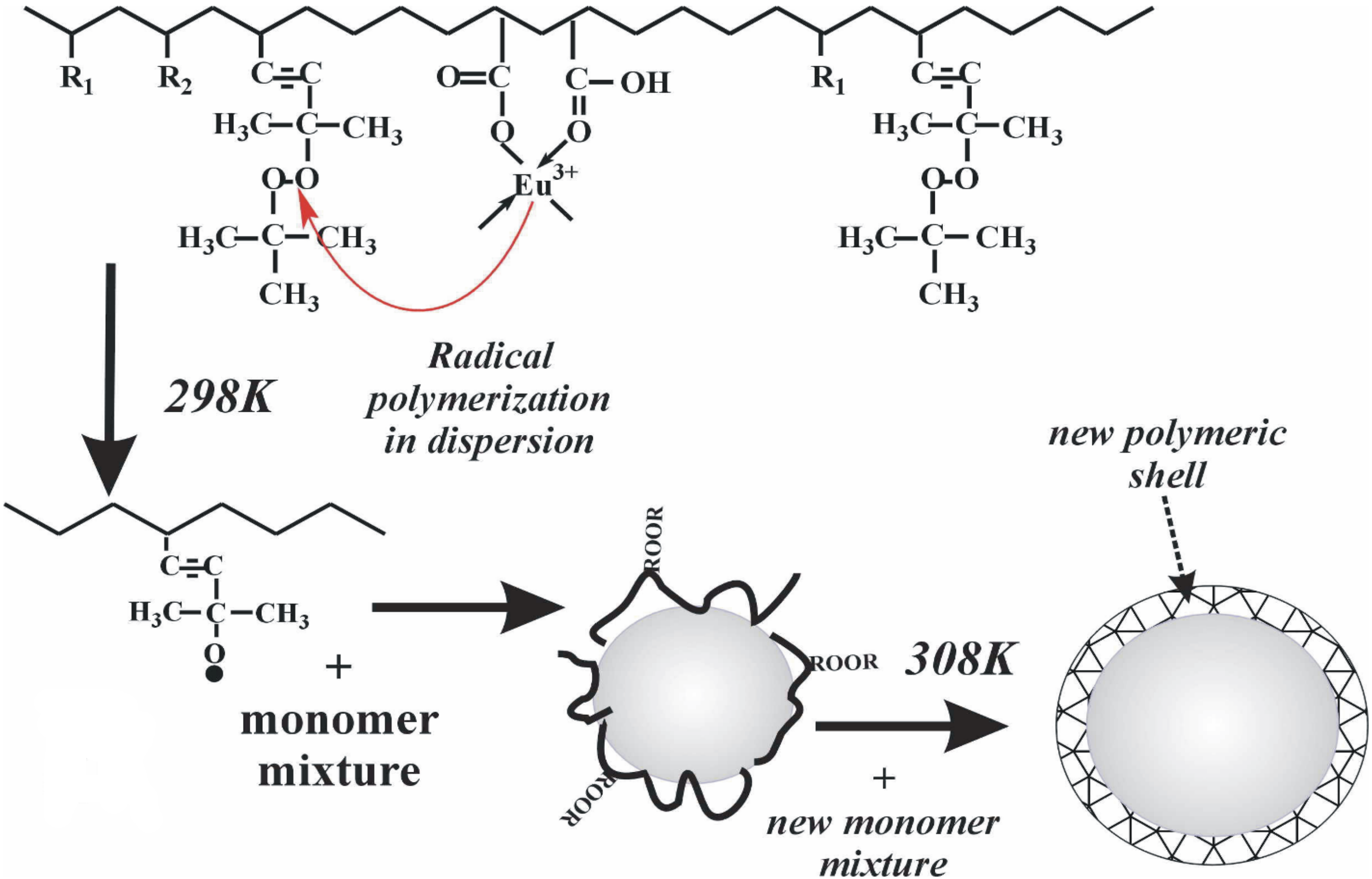

The scheme of the synthesis and functionalization of luminescent polymer NPs

I.1. Coordinating complexes of rare earth elements with oligoperoxide ligands (OMC) and polymeric nanoparticles synthesized via water dispersion polymerization initiated by OMC.

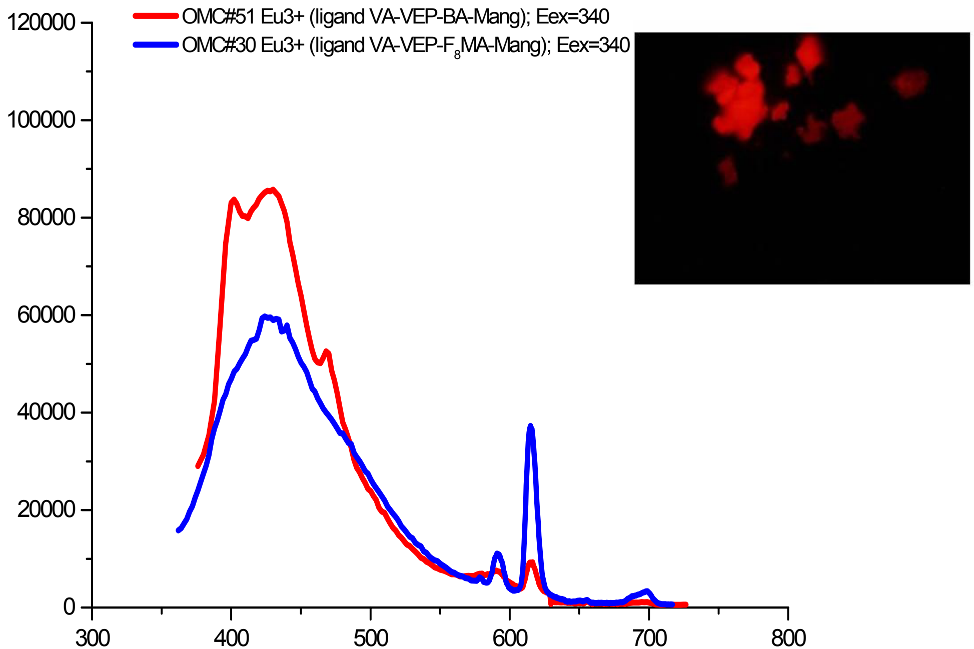

Spectra of luminescence of oligoperoxide metal complexes with Eu^{3+} on the basis copolymer of vinyl acetate (VA), VEP, maleic anhydride (MA) (1) and VA, VEP, MA and fluoro acrylate (2)

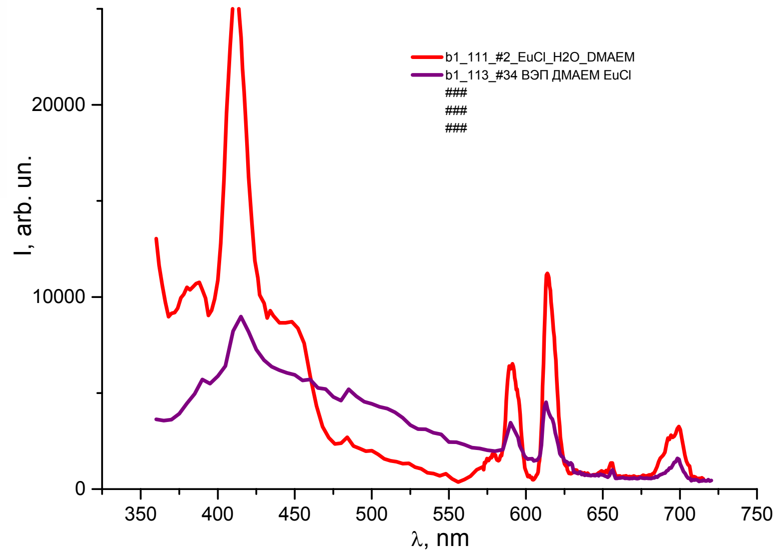

Spectra of luminescence of Eu^{3+} salt of oligoperoxide acrylonitrile (AN), VEP, dimethylaminoethyl methacrylate (DMAEM) (1) and VA, VEP DMAEM (2)

I.1. Coordinating complexes of rare earth elements with oligoperoxide ligands (OMC) and polymeric nanoparticles synthesized via water dispersion polymerization initiated by OMC.

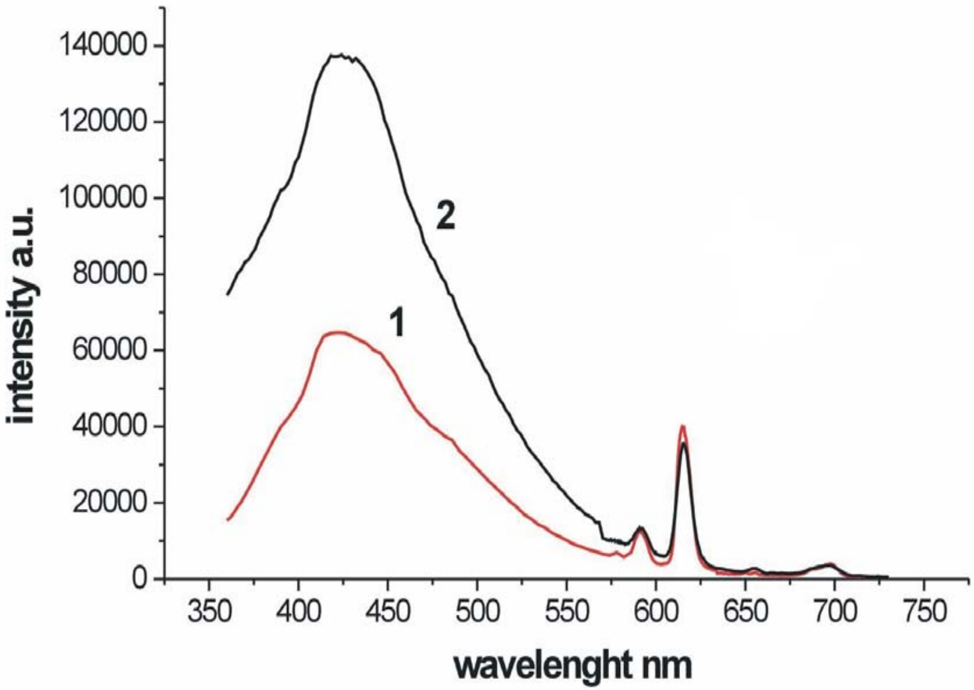

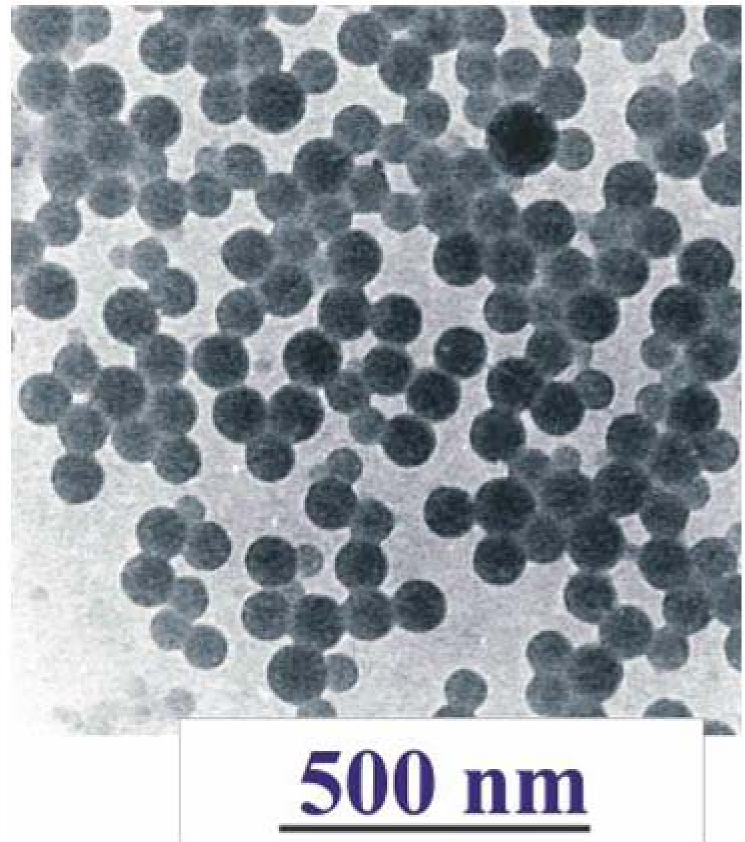

Luminescence spectrum (b) of Eu^{+3} containing OMC (1) and polymer NPs (2) synthesized in the presence of OMC; TEM images of luminescent NPs (c).

I.2. Synthesis of oligoperoxide and oligoelectrolyte surfactants containing luminescent organic fragments.

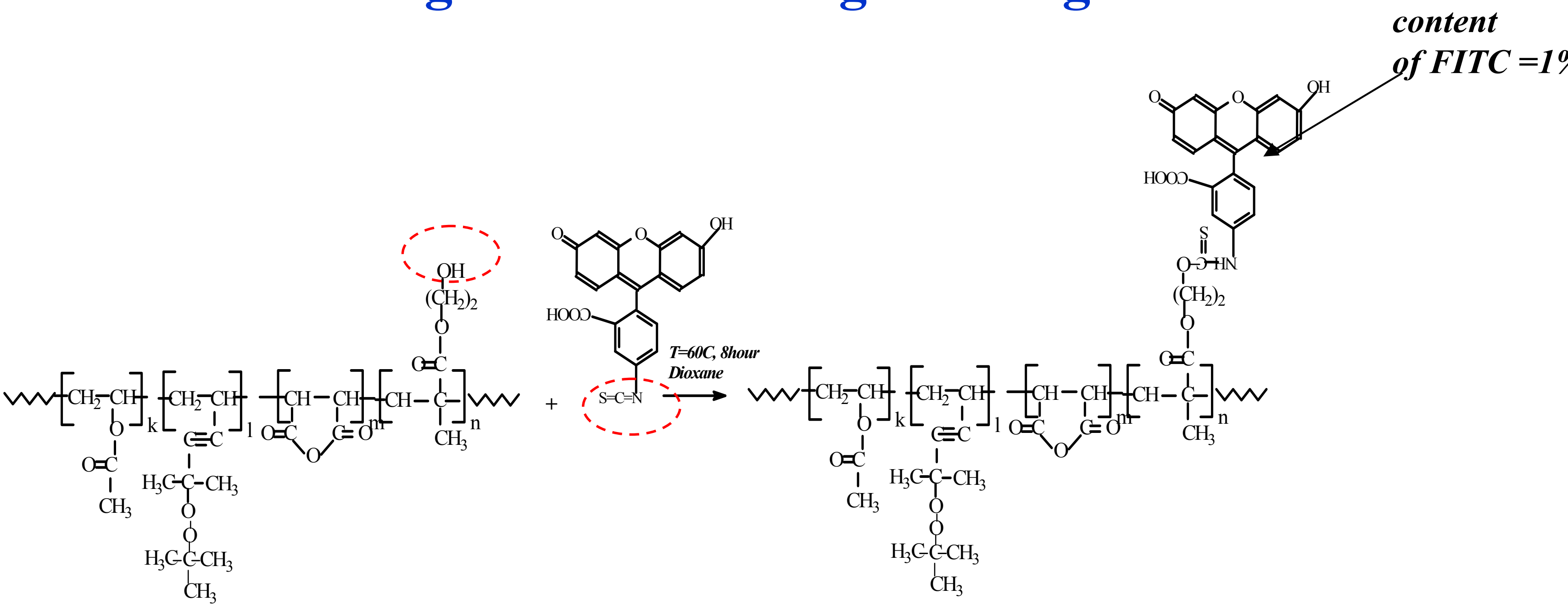

I.2. Synthesis of oligoperoxide and derived oligoelectrolyte surfactants containing luminescent organic fragments.

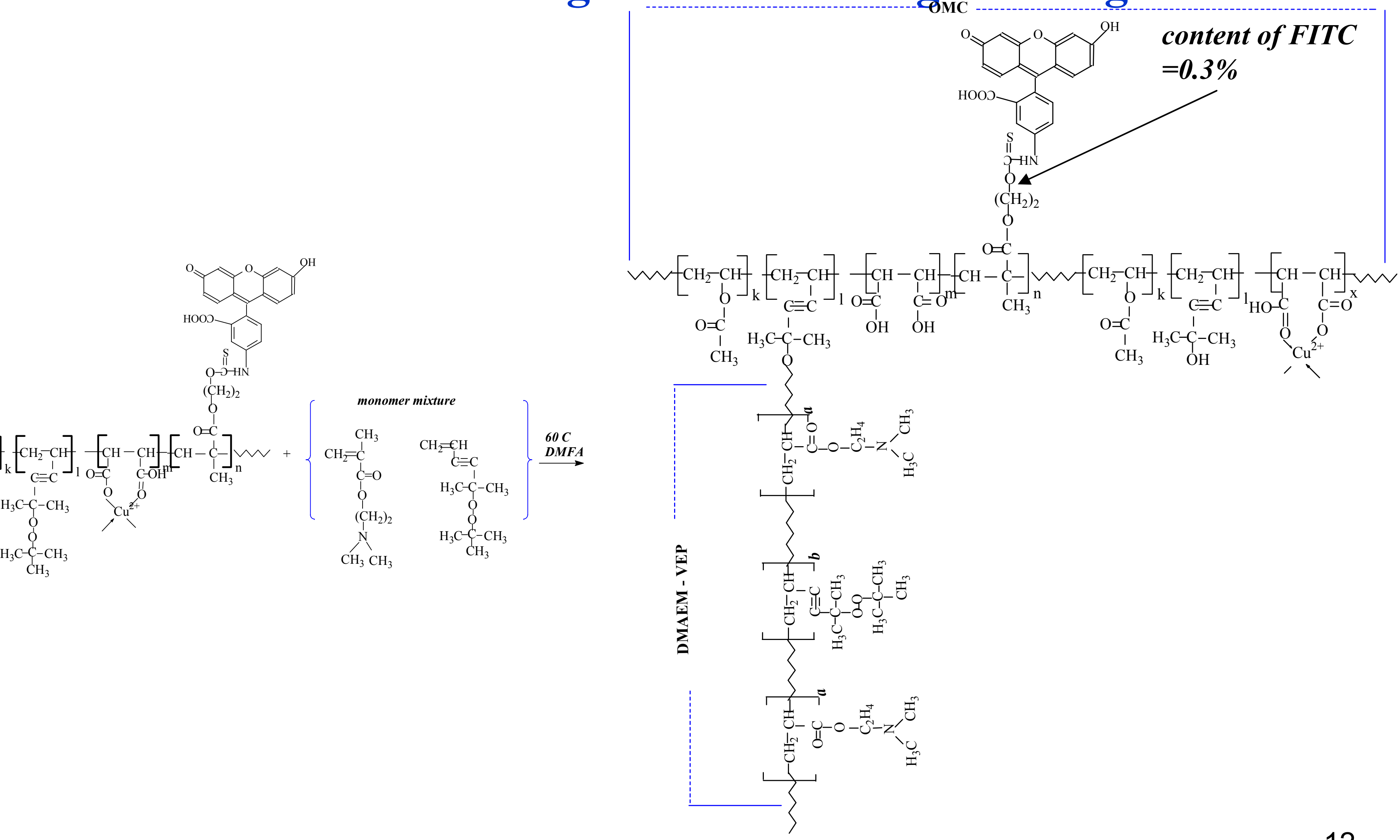

I.2. Synthesis of oligoperoxide and oligoelectrolyte surfactants containing luminescent organic fragments.

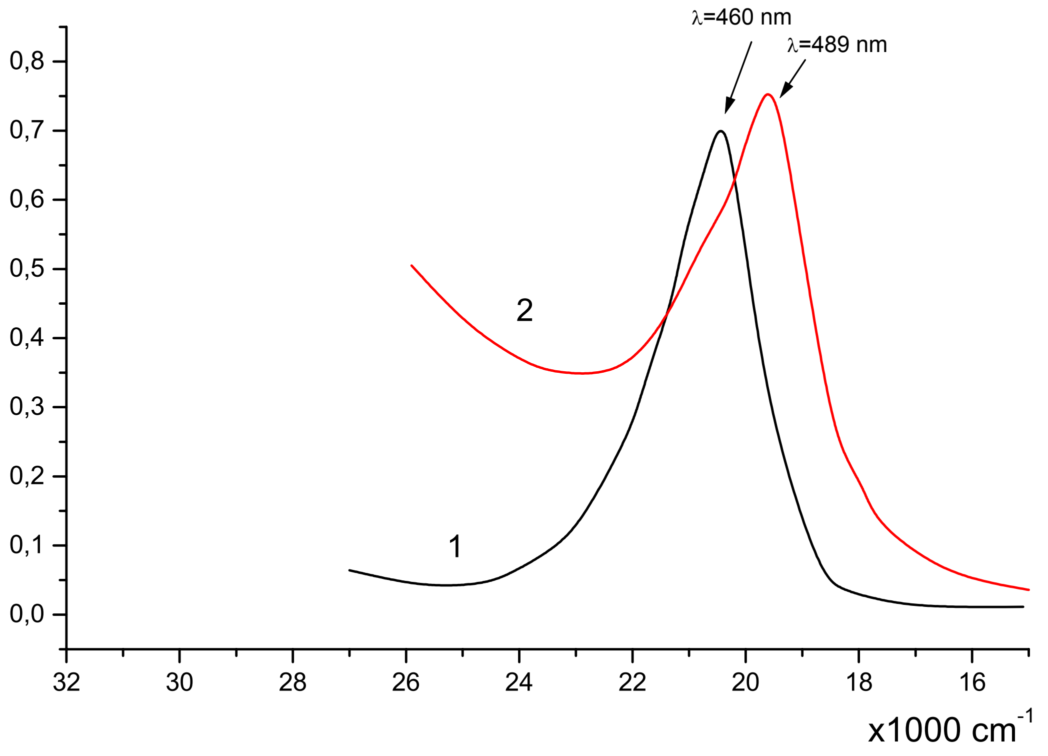

UV-spectra of FITC (1) and comb- like copolymer with FITC fragments (2) in **water solutions**

I.2. Synthesis of oligoperoxide and derived oligoelectrolyte surfactants containing luminescent fragments as a result of reactions with reactive phosphors.

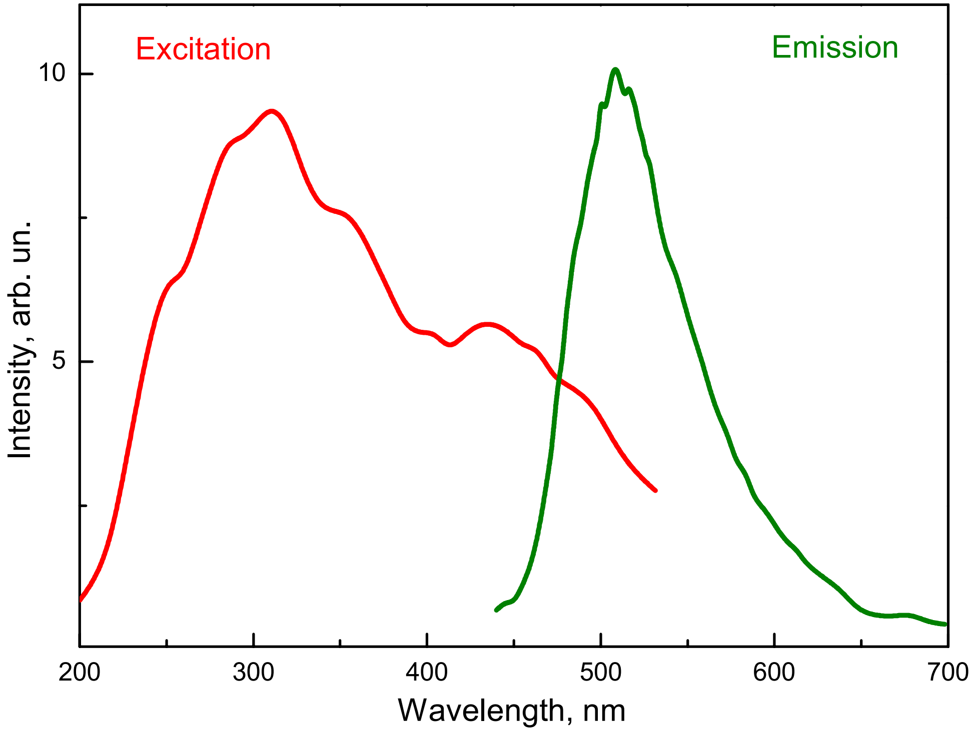

The excitation and emission spectra of VA-VEP-MA-HEMA+FITC-graft-VEP-DMAEM branched copolymer

I.3. Micelle-like assemblies formed by oligoperoxide or oligoelectrolyte surfactants solubilizing organic phosphors in hydrophobic core.

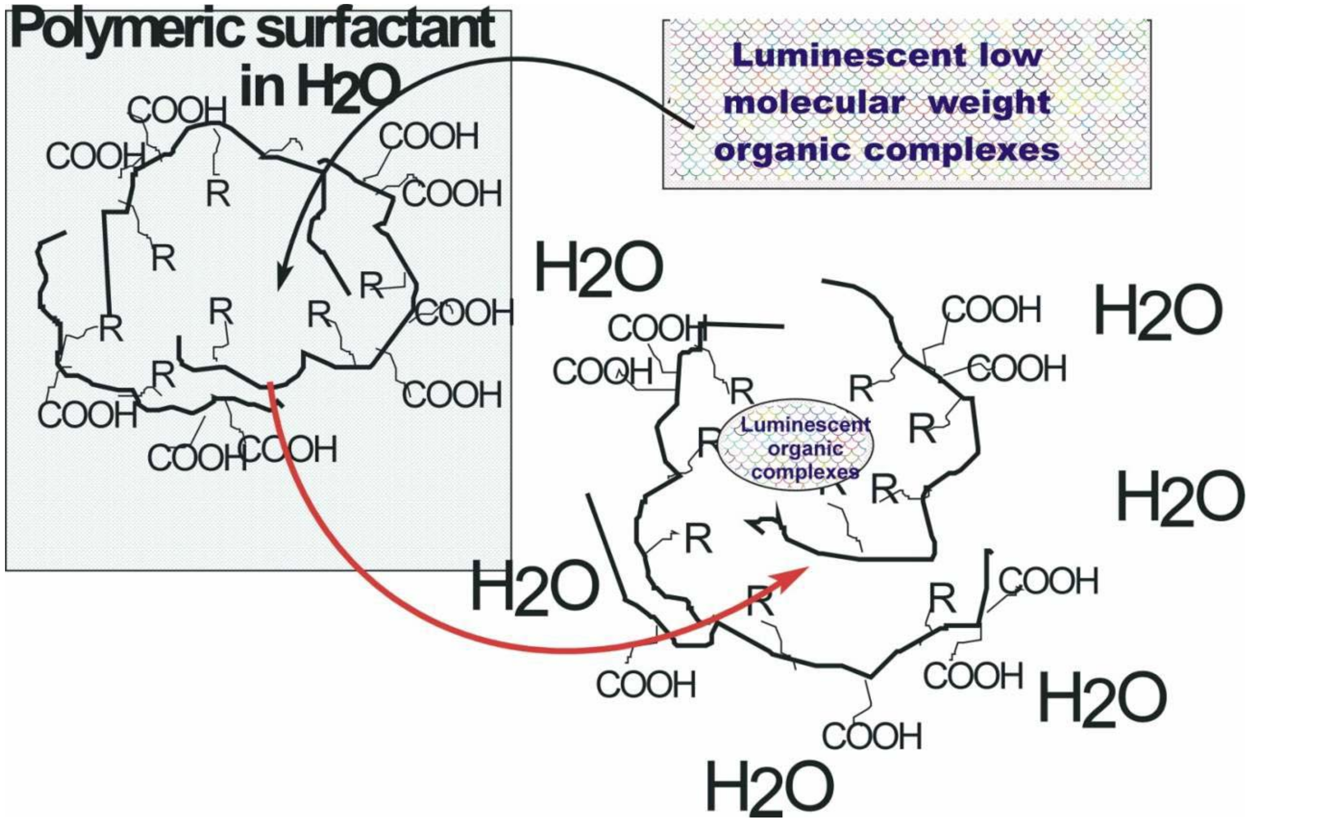

Scheme of solubilization of water-insoluble organic phosphors in the core of micelle forming oligoperoxide surfactants in water

I.3. Micelle-like assemblies formed by oligoperoxide or oligoelectrolyte surfactants containing organic phosphors in hydrophobic core.

Coordinating metal complex was synthesized by prof. S. Meshkova, Bogatskiy Physico-Chimical Institute of NASU

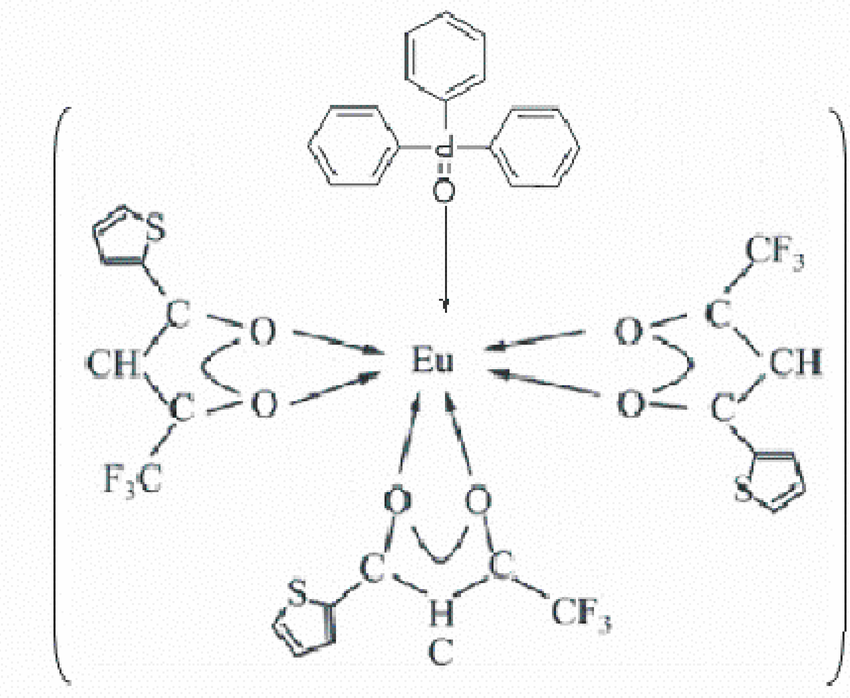

Eu $(TTA)_3$TFFO, where TTA - thenoyltrifluoroacetone, TFFO - triphenylphosphineoxide

I.3. Micelle-like assemblies formed by oligoperoxide or oligoelectrolyte surfactants solubilizing organic phosphors in hydrophobic core.

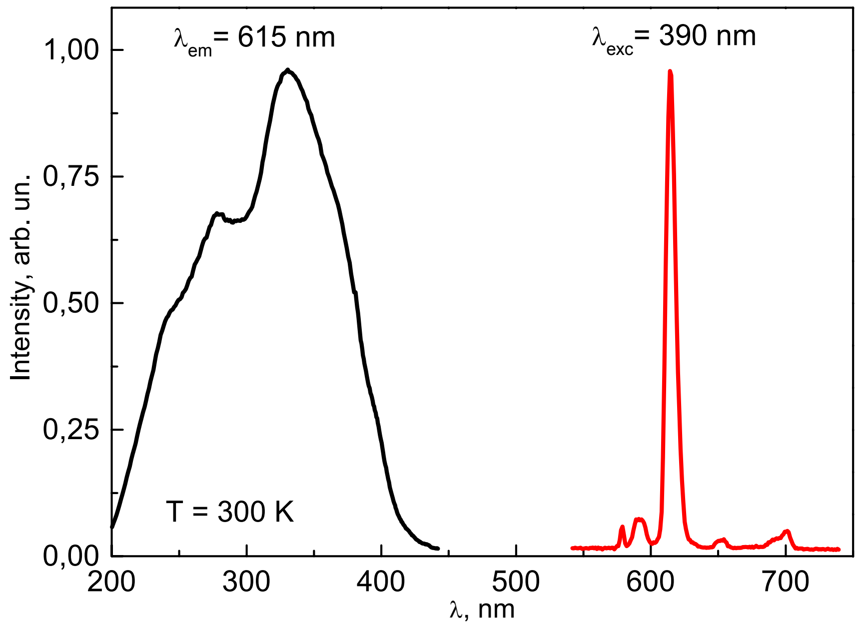

The excitation and emission spectra of Eu^{3+} for Eu (TTA) in the micelle hydrophobic zones of oliogoperoxide surfactants

I.4. Oligoelectrolyte based nanogels containing coordinating rare earth cations or organic phosphors in the pores.

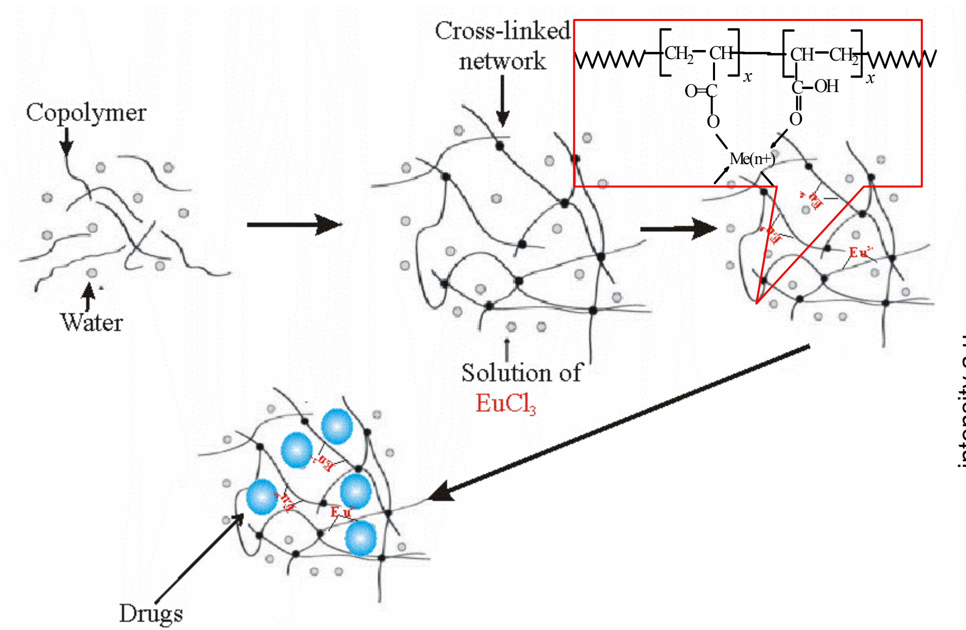

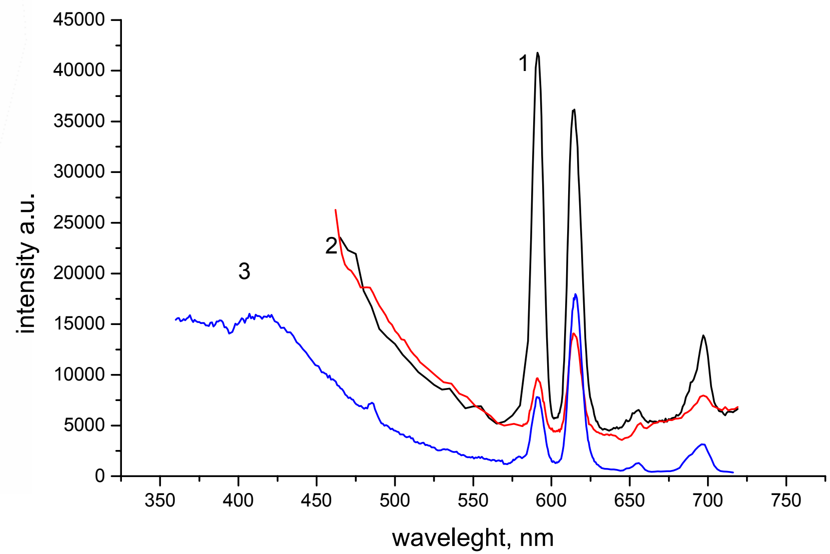

The scheme of the formation of luminescent carboxyl-containing gel carriers and loading poor water soluble drugs

Luminescent spectrum of coordinatung complex of Eu^{3+} with carboxyls of nanogel. Excitation at 397nm (1); 387nm - (2); 300nm – (3).

I.4. Oligoelectrolyte based nanogels containing coordinating rare earth cations or organic phosphors in the pores.

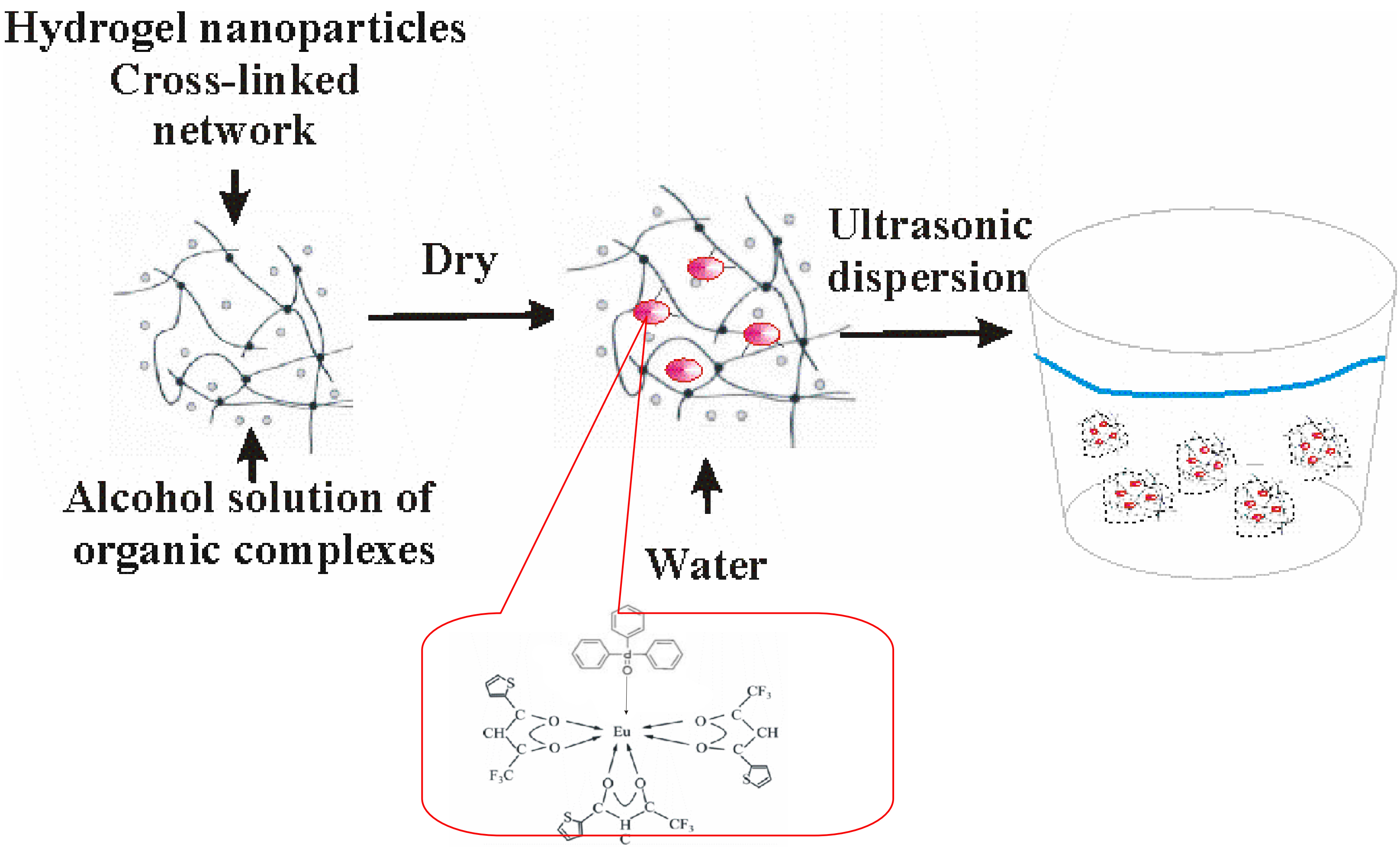

I.4. Oligoelectrolyte based nanogels containing coordinating rare earth cations or organic phosphors in the pores.

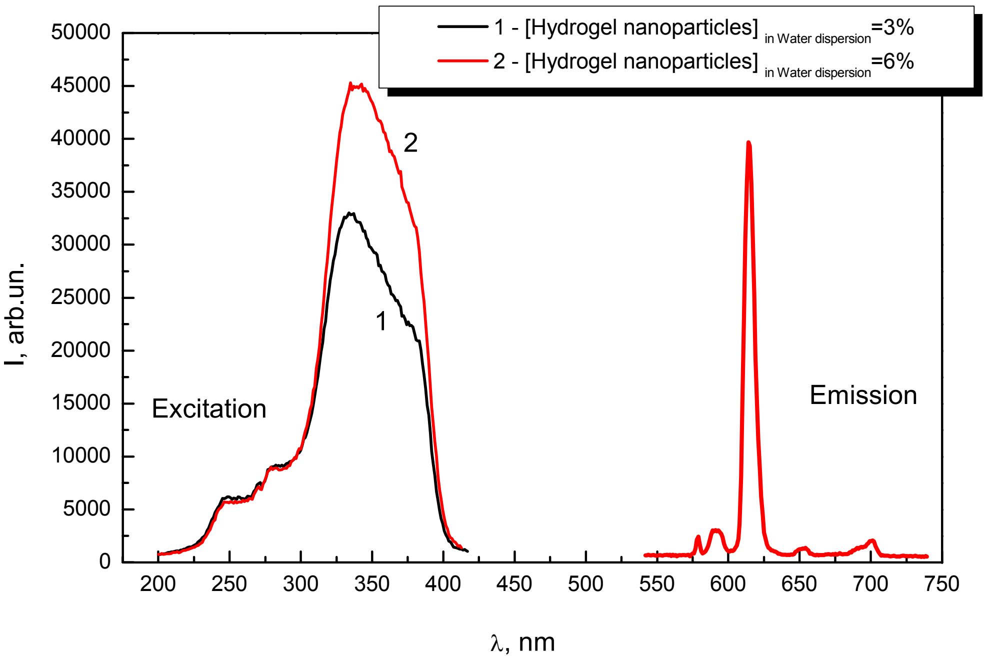

The excitation and emission spectra of nanogel water dispersions with the adsorbed complex Eu (TTA) 3TFFO, [nanogel]=3%(1) and 6% (2)([Eu (TTA)3·TFFO] =1% per nanogels)

Water dispersions of nanogels containing 3% (a), 1% (b), 0.5% (c) of complex Eu(TTA)$_3$TFFO

I.4. Oligoelectrolyte based nanogels containing coordinating rare earth cations or organic phosphors in the pores.

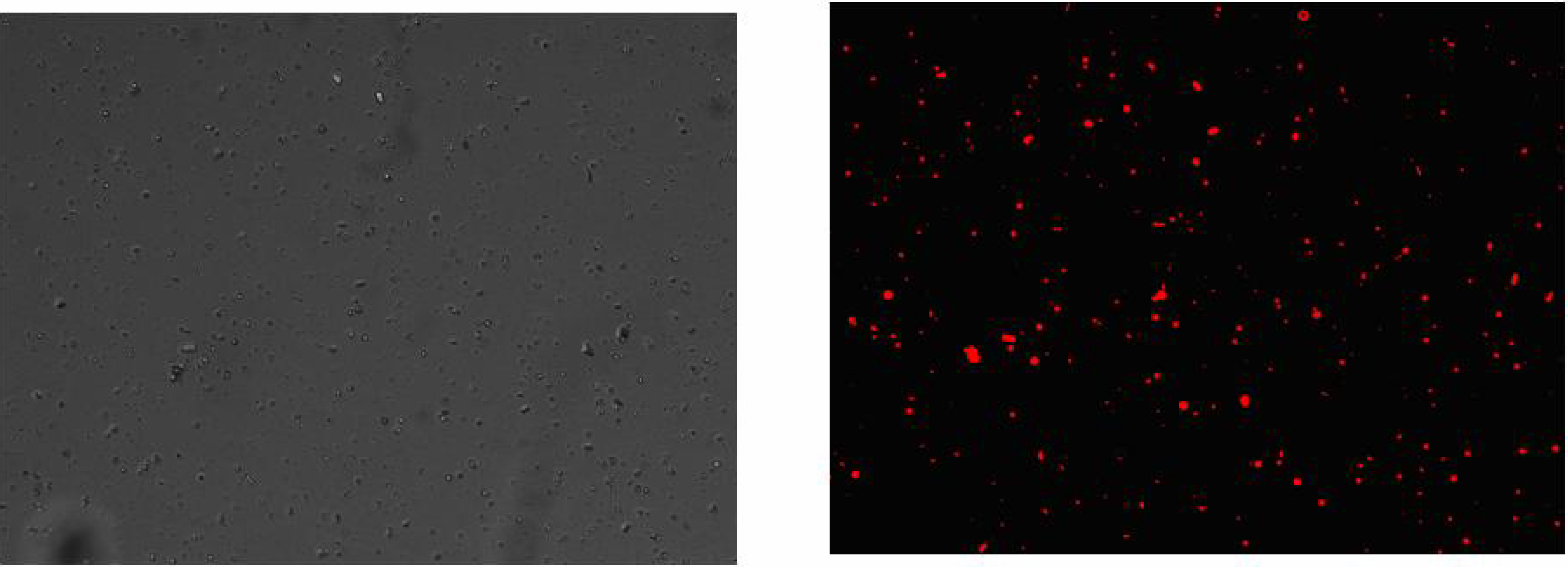

Optical microscope images of nanogels containing luminescent complex Eu (TTA)3·TFFO a) differential-interferential contrast, b) fluorescence

I.5. Encapsulation of phosphors in the core of functional polymeric nanoparticles via water dispersion polymerization.

Surface - active monomer (SAM)

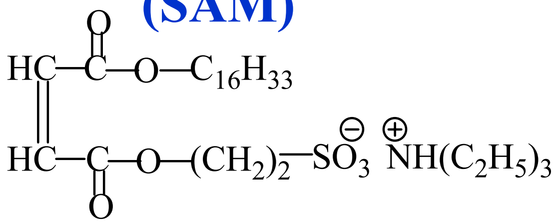

OMC

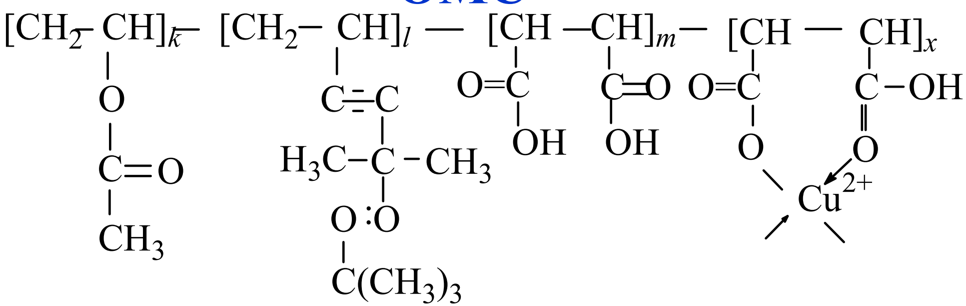

Fluorescent dyes

Water soluble

Fluorescein

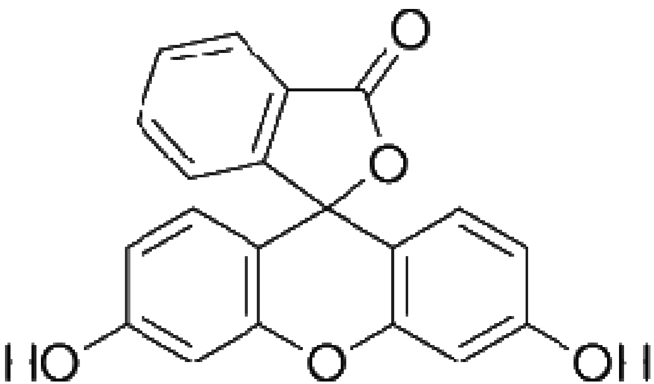

Water insoluble

2,6-Di-tert.-butyl-4-(2,5-diphenyl-3,4-dihydro-2H-pyrazol-3-yl)-phenol (pyrazolyne)

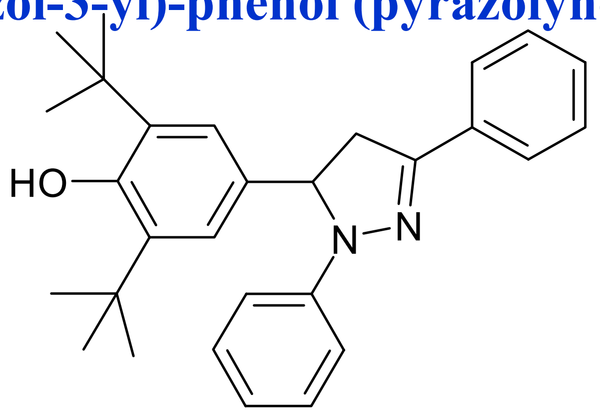

I.5. Encapsulation of phosphors in the core of functional polymeric nanoparticles via water dispersion polymerization.

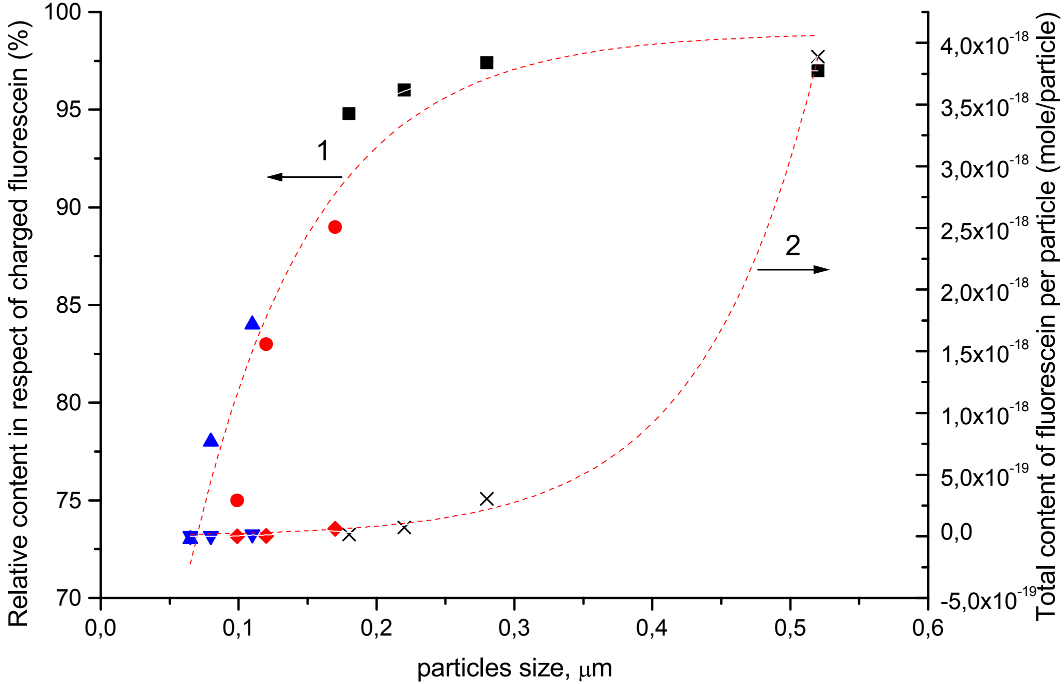

The dependences of relative in respect of charged amount (1) and total (2) contents of fluorescein encapsulated per one functional nanoparticle on nanoparticle size. (■,×– monomer mixture: STR:SAM, initiator – PA, ●,♦– monomer mixture: STR:SAM, initiator – OMC, ▲,▼– monomer mixture: MMA-BA-GMA:SAM, initiator – OMC)

I.5. Encapsulation of phosphors in the core of functional polymeric nanoparticles via water dispersion polymerization.

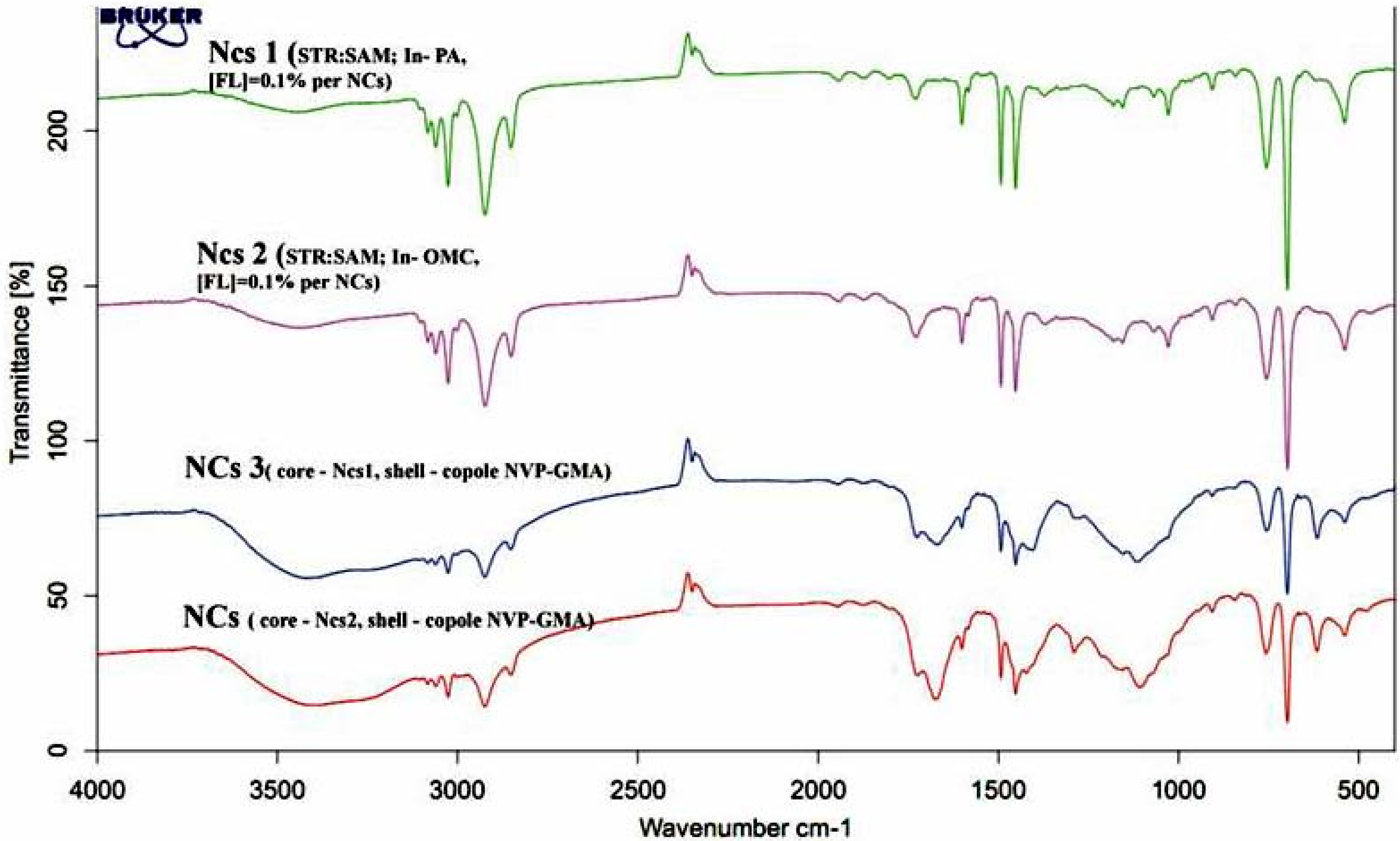

FT-IR spectrum of polymeric NPs containing encapsulated fluorescein, copolymer of St and SAM (1, 2) and core-shell type NPs (3,4)

I.5. Encapsulation of phosphors in the core of functional polymeric nanoparticles via water dispersion polymerization.

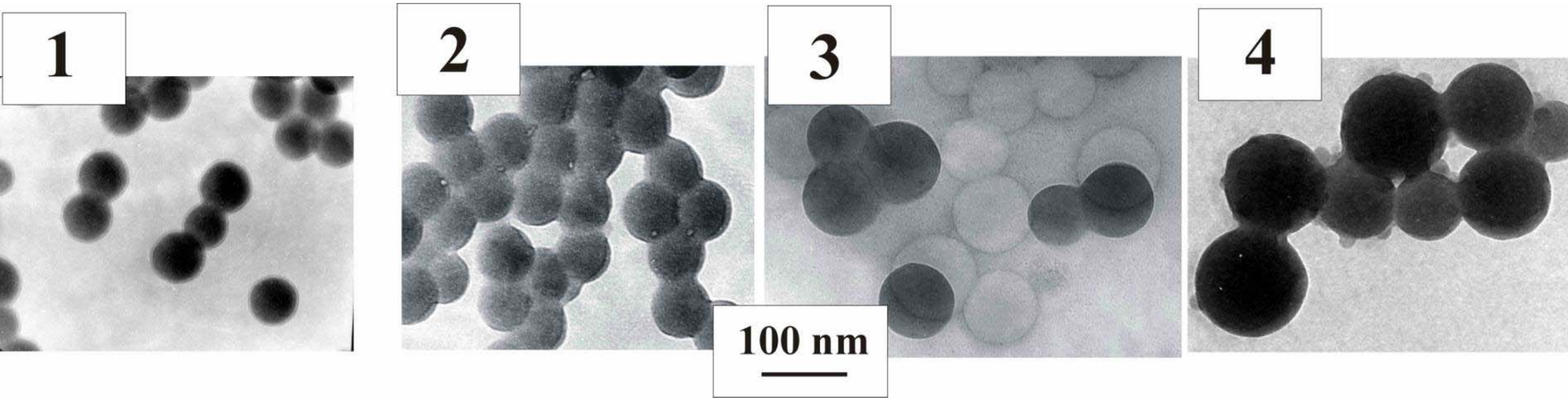

TEM images of functional polymeric NPs synthesized via water dispersion polymerization of styrene with SAM at St: SAM ratio 90:10 initiated by OMC: 1 – without fluorescein (FL), 2 – [FL] =0.1% per St, 3 – [FL] =0.5% per St, and initiated by PA, [FL] =0.1% per St (3)

I.5. Encapsulation of phosphors in the core of functional polymeric nanoparticles via water dispersion polymerization.

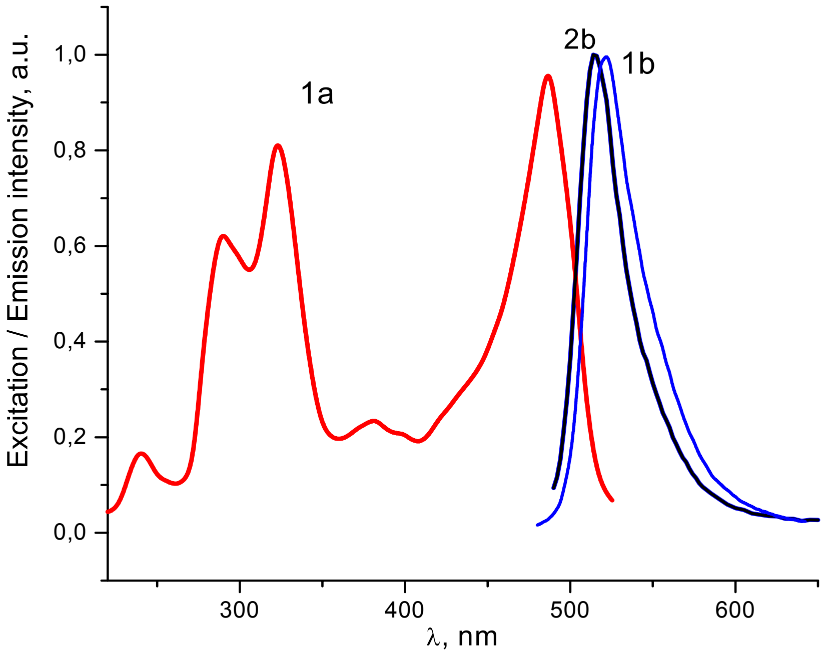

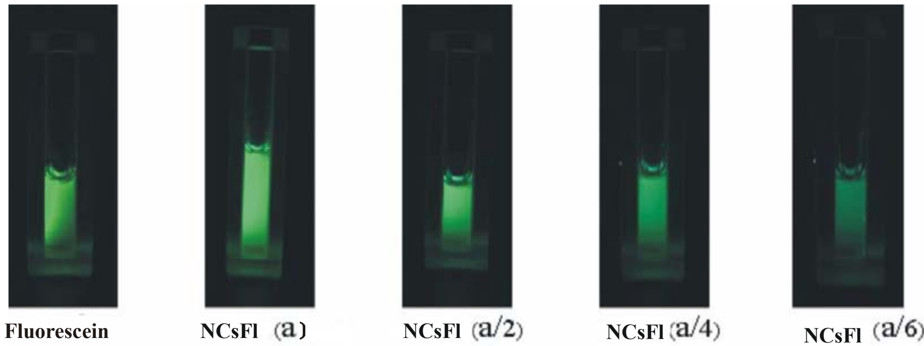

Fluorescence (1) and fluorescence excitation (2) spectra of polymeric fluorescein-encapsulated NPs. b – Emission spectra of fluorescein (1) and of fluorescein-encapsulated NPs (2); excitation at 425 nm.

Green fluorescence of fluorescein and FITC-encapsulated polystyrene nanoparticles (PSFITS a) in water based systems at distinct dilution (PSFITS a/2, a/4, a/6)

I.6. Functional mineral nanoparticles of $LaPO_4$, $LuPO_4$, $LuBO_3$, GdF_3, CaF_2, BaF_2 core doped with cations of Pr^{+3}, Ce^{+3}, Eu^{+2}, Eu^{+3}.

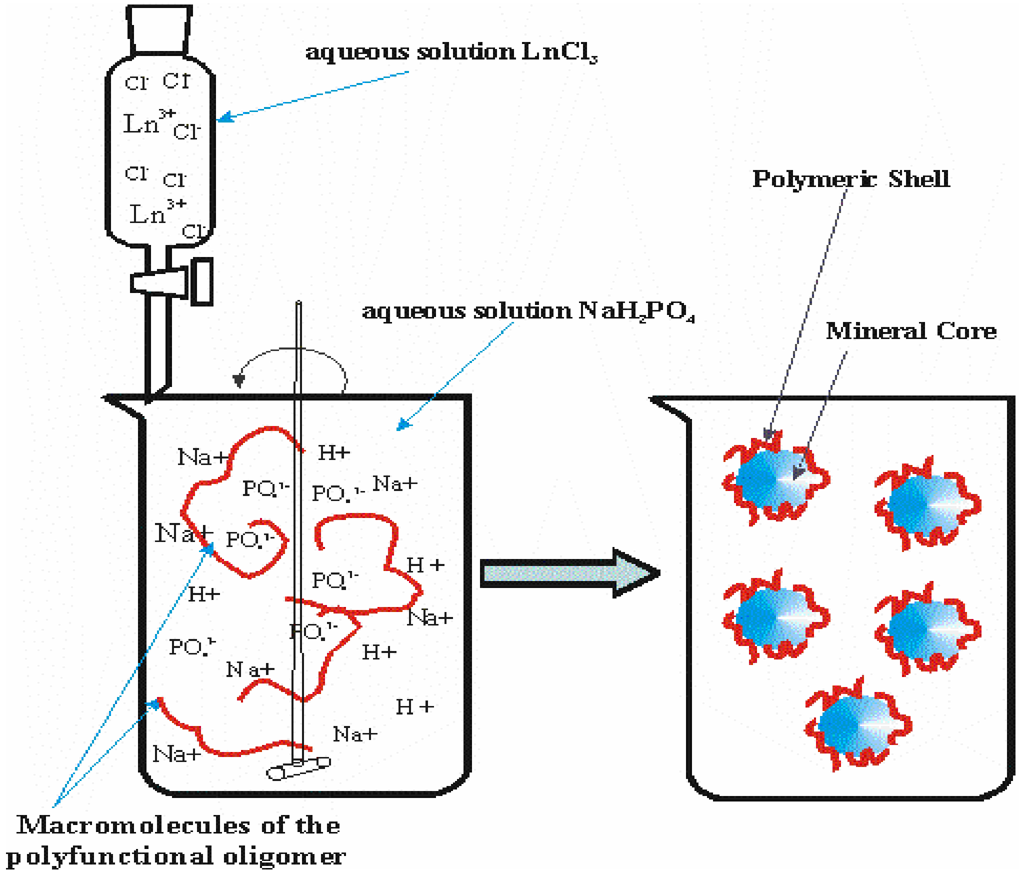

The scheme of the lantanide nanoparticle template synthesis

I.6. Functional mineral nanoparticles of $LaPO_4$, $LuPO_4$, $LuBO_3$, GdF_3, CaF_2, BaF_2 core doped with cations of Pr^{+3}, Ce^{+3}, Eu^{+2}, Eu^{+3}.

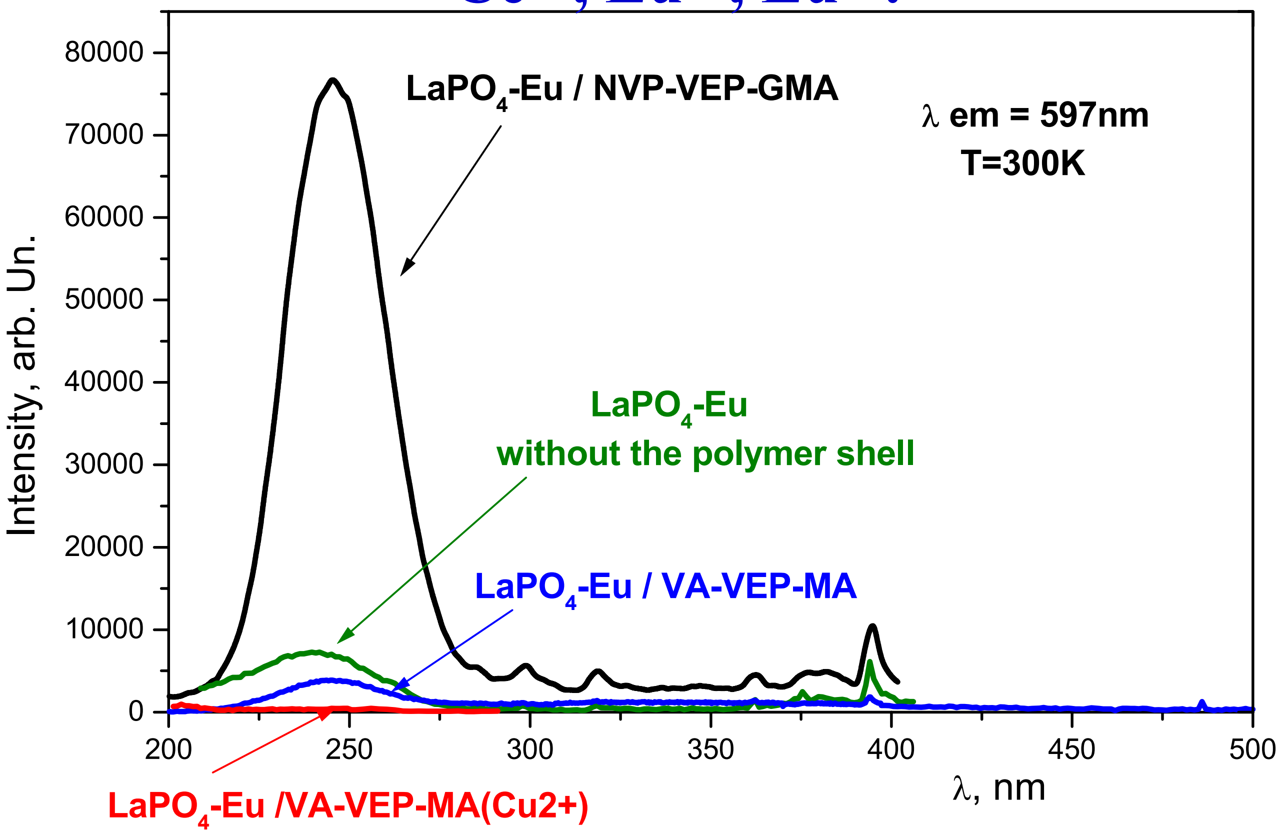

Influence of the nature of oligoperoxide shell on the surface of nanoparticles on intensity of their luminescence

I.6. Functional mineral nanoparticles of $LaPO_4$, $LuPO_4$, $LuBO_3$, GdF_3, CaF_2, BaF_2 core doped with cations of Pr^{+3}, Ce^{+3}, Eu^{+2}, Eu^{+3}

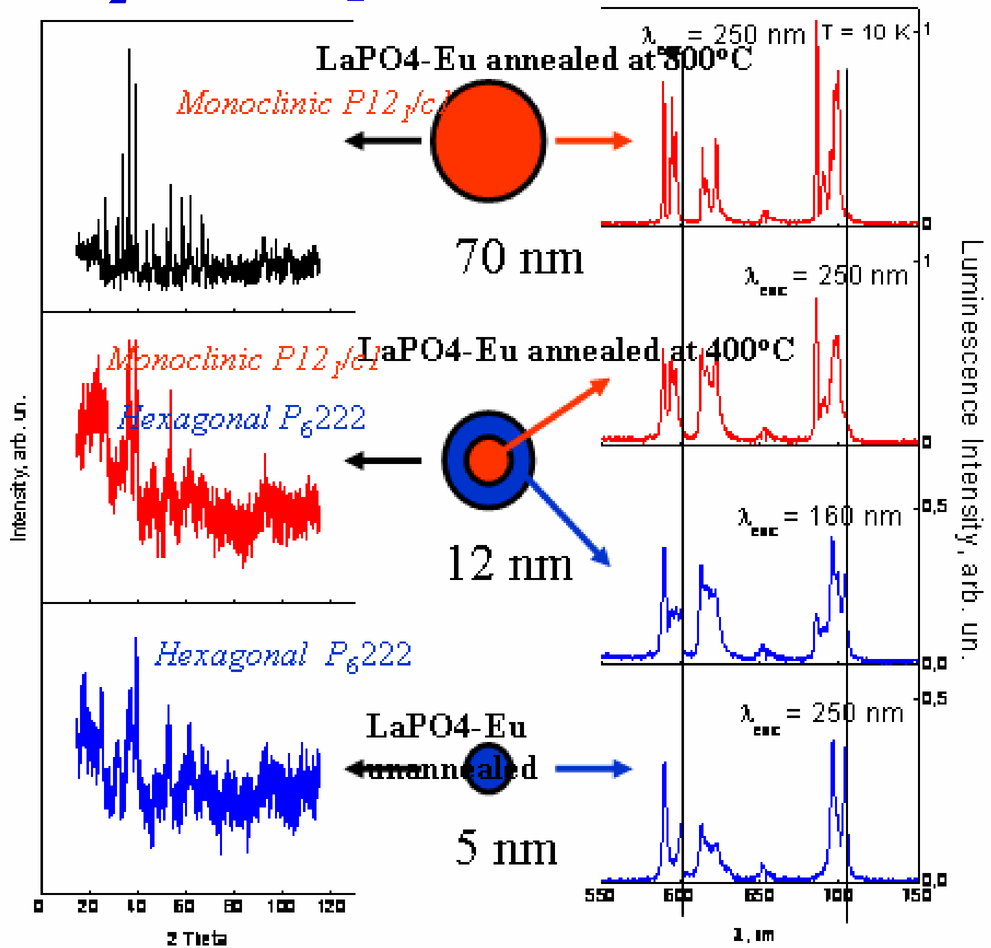

X-Ray patterns of nanoparticles $LaPO_4$-Eu

The luminescence spectra of nanoparticles $LaPO_4$-Eu; T=10 K.

X-ray patterns of $LaPO_4$…Eu^{3+} nanoparticles annealed at different temperature (a) and spectrum of their luminescence (b): hexagonal lattice (blue) and monoclinic lattice (red)

I.6. Functional mineral nanoparticles of $LaPO_4$, $LuPO_4$, $LuBO_3$, GdF_3, CaF_2, BaF_2 core doped with cations of Pr^{+3}, Ce^{+3}, Eu^{+2}, Eu^{+3}

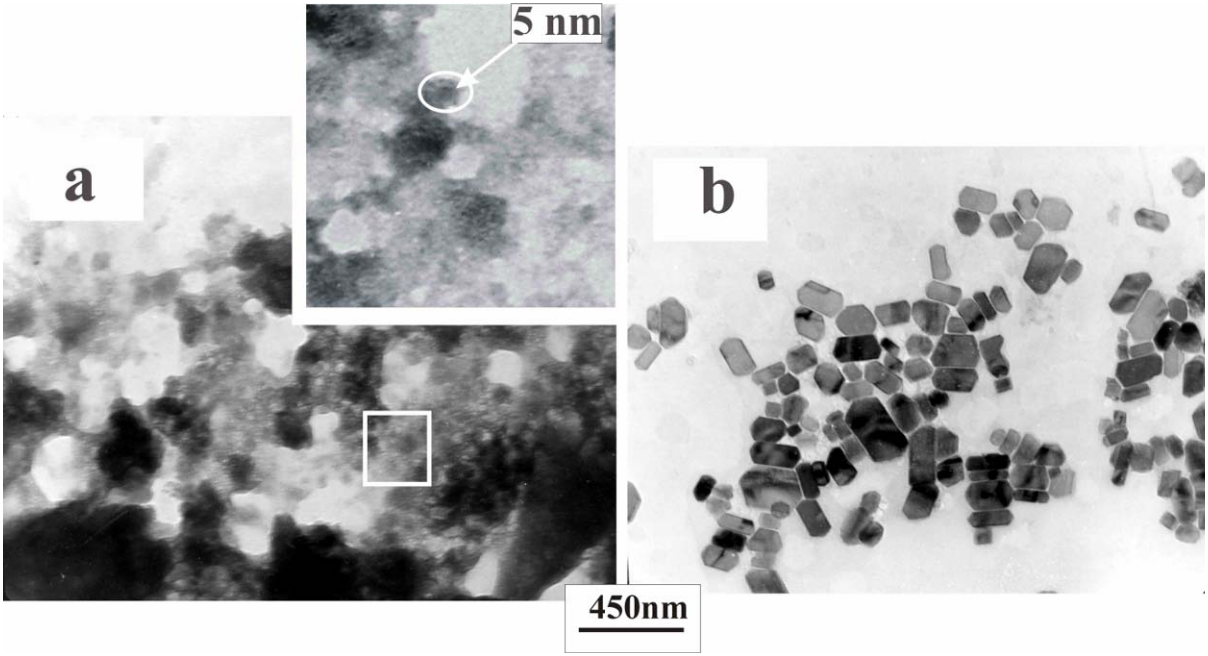

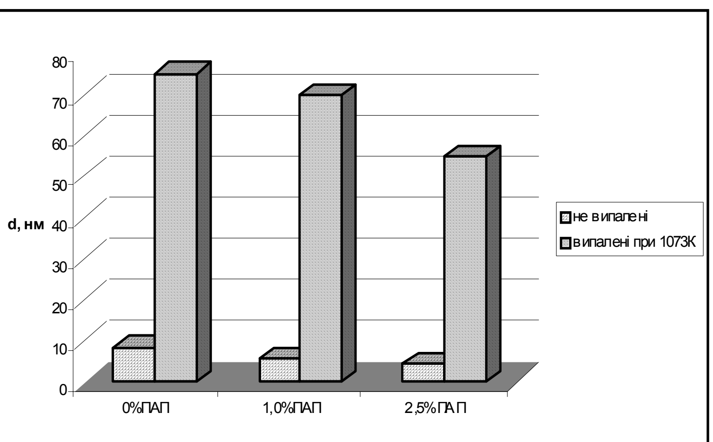

The dependence of the size of $LaPO_4$…Eu^{3+} nanoparticles non annealed and annealed on oligoperoxide surfactant concentration in the solution during their nucleation

I.6. Functional mineral nanoparticles of $LaPO_4$, $LuPO_4$, $LuBO_3$, GdF_3, CaF_2, BaF_2 core doped with cations of Pr^{+3}, Ce^{+3}, Eu^{+2}, Eu^{+3}

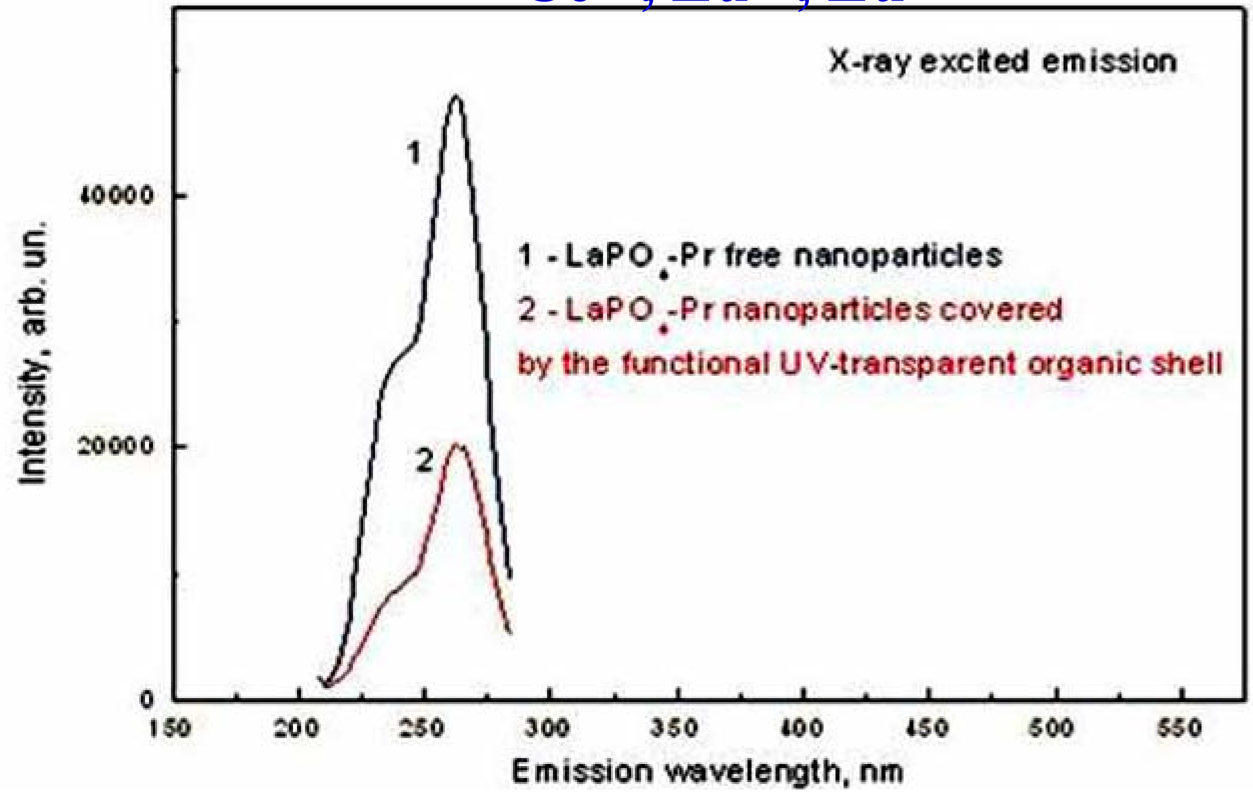

Spectrum of X-ray excited nanoparticles $LaPO_4$…Pr annealed at 800C (1) and the same nanoparticles after adsorption activation with oligoperoxide surfactant and subsequent radical grafting polystyrene shell (2)

Why such oligoperoxide based luminescent nanocomposites and nanolayers?

- Controlled particle size and size distribution
- Controlled functionality and reactivity
- Controlled physically detectable characteristics of nanocomposites and nanoshells
- Presence of peroxide links on particle surface provides tailored particle functionalization (epoxide, aldehyde, maleimide etc.) via graft copolymerization.
- Availability of controlled reactive functionality on nanoparticle surface provides attachment of cell recognizing biological vectors (saccharides, lectins, antibodies).

32

II. Cellular studies and potential biomedical application for cell detection, tagging and treatment.

*** Cellular study was fulfilled in Lviv Institute of Cell Biology under the guidance of Professor R. Stoika**

II. Cellular studies and potential biomedical application for pathological cell detection, tagging and treatment.

Labeling dying cell by fluorescein-encapsulated functional nanoparticles

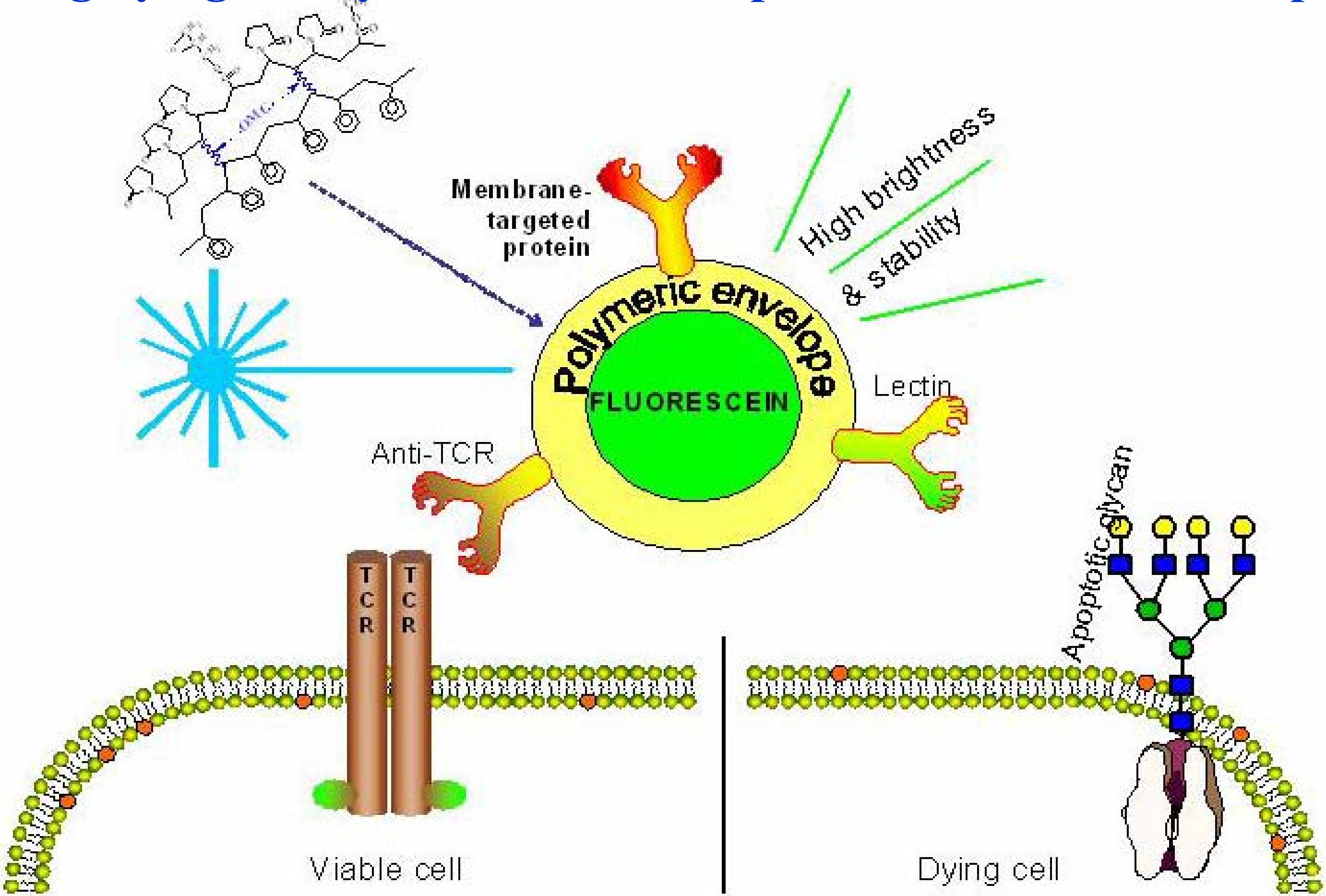

II. Cellular studies and potential biomedical application for pathological cell detection, tagging and treatment.

Targeted biodegradation of polymeric nanoconjugates

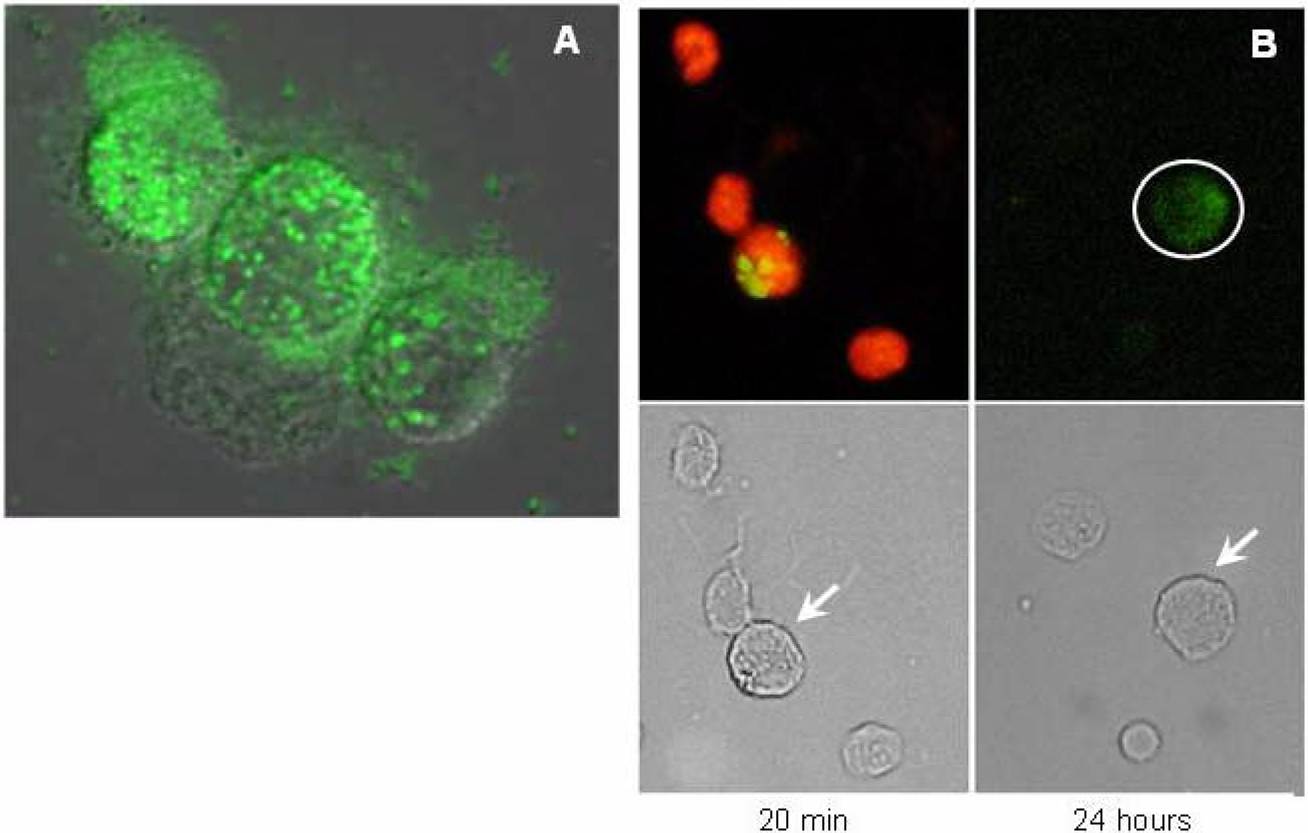

A - BSA-conjugated fluorescein-containing nanoparticles (~200 nm) are bound to murine macrophages of J774.2 line after 20 min incubation. DIC with superimposed fluorescent image. B – Ig-conjugates fluorescein-containing nanoparticles (~300 nm) were injected into the peritoneal cavity of mice. After 20 min and 24 h, peritoneal cells were removed, washed, concentrated and studied. Top panel – fluorescent microscopy; lower panel – light microscopy. Macrophages (indicated by arrow) were identified on the basis of their morphology and propidium iodine (20 min, red color) or DAPI counterstaining (not shown). Note that after 24 h NPs were digested by the macrophages

II. Cellular studies and potential biomedical application for pathological cell detection, tagging and treatment.

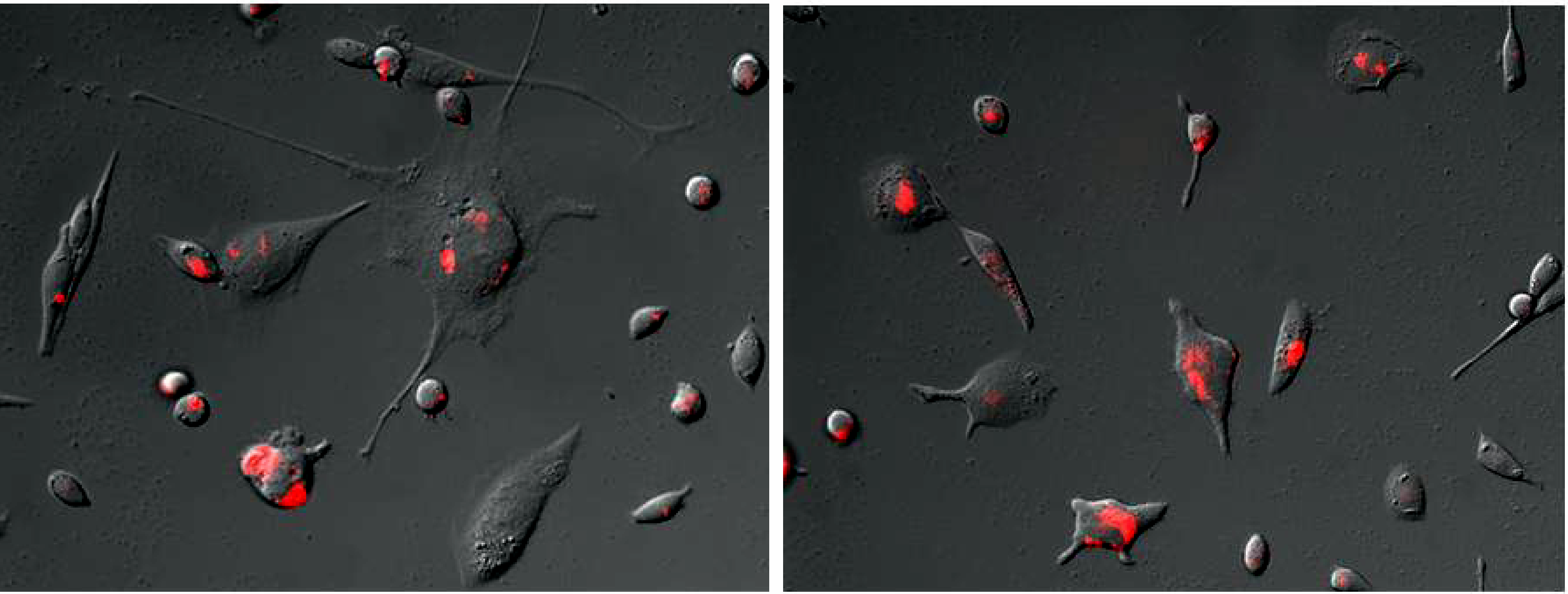

a

b

Engulfment of functional oligoelectrolyte based nanogels filled with complex Eu(TTA)$_3$ TFFO by melanoma cells; concentration of nanogels in water dispersion – 0.1%, a) 1 microliter per 1 ml of cultural medium; b) 10 microliter per 1 ml of cultural medium (incubation 24h)

II. Cellular studies and potential biomedical application for pathological cell detection, tagging and treatment.

a b

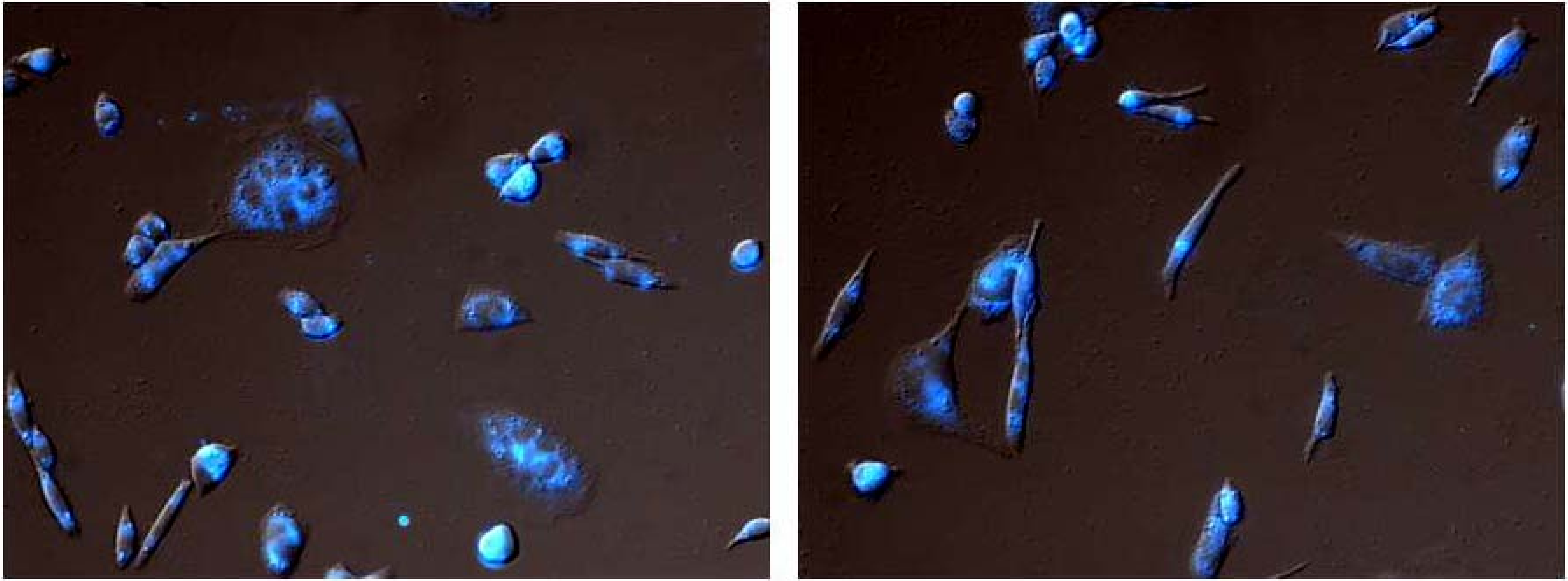

Engulfment of pyrazolyn-containing functional polymeric nanoparticles by melanoma cells; concentration of nanparticles in water dispersion – 0.1%, a) 1 microliter per 1 ml of cultural medium; b) 10 microliter per 1 ml of cultural medium (incubation 24h)

II. Cellular studies and potential biomedical application for pathological cell detection, tagging and treatment.

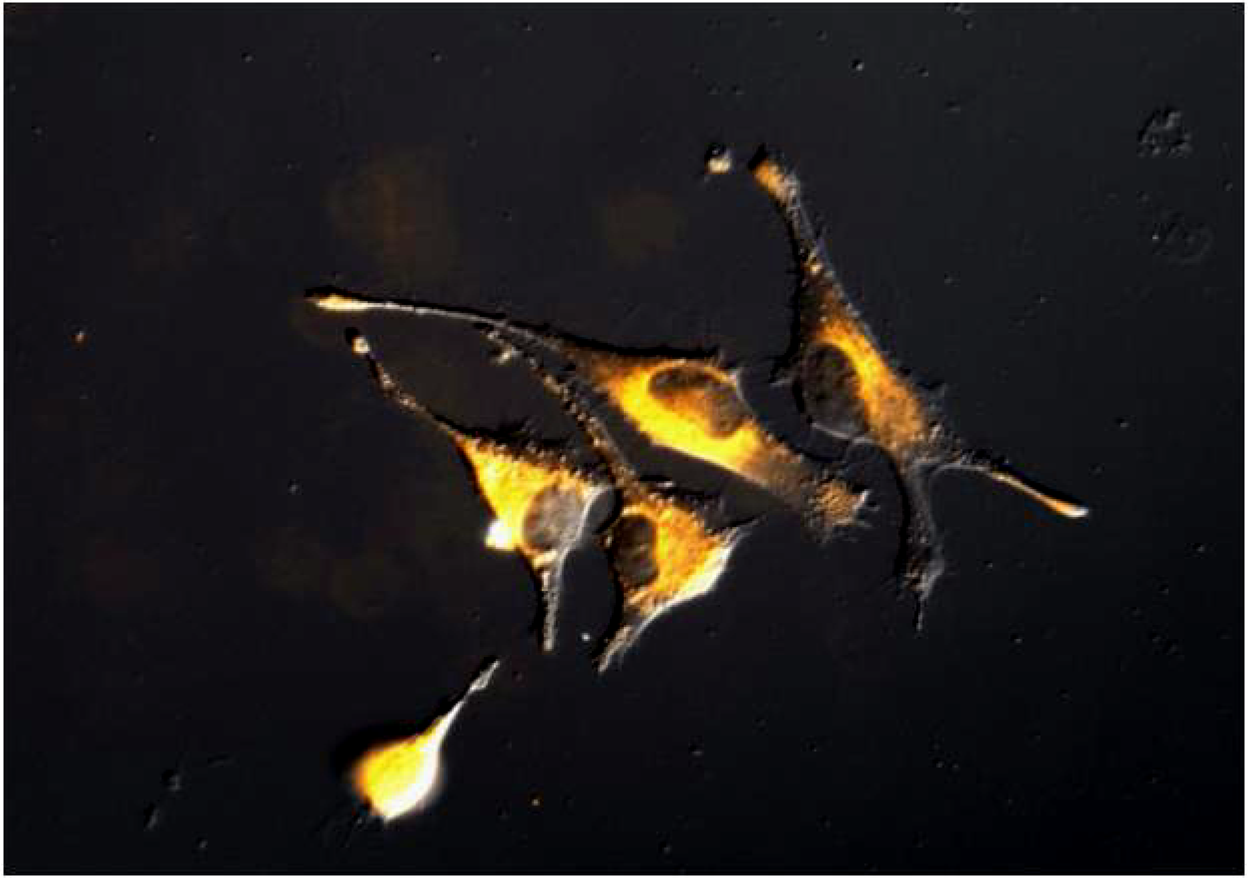

Engulfment of functional nanosized scintillators based on $LaPO_4$…Eu by human melanoma cells line SK-MEL-28.

Acknowledgements

Many thanks to my team and partners

Dr. N. Mitina, Dr. O. Hevus, Dr. O. Shapoval, PhD students O. Myagkota from Lviv Polytechnic National University;

Professor A. Voloshinovskii, Professor A. Gektin, Dr. P. Zhmurin, Dr. V. Vistovskiy from I. Franko National University and Kharkiv Institute of Scintillation Materials of NASU

Professor R. Stoika, Dr. R. Bilyy, Dr. R. Panchuk and team from Cell Biology Institute of NASU

for the experimental work as well as for the collaboration, ideas and discussion